MOX–Report No. 04/2013

Stent deformation, physical stress, and drug elution obtained with provisional stenting, conventional culotte and Tryton-based culotte to treat bifurcations: a virtual simulation study

Morlacchi, S.; Chiastra, C.; Cutr, E.; Zunino, P.; Burzotta, F.; Formaggia, L.; Dubini, G.; Migliavacca, F.

MOX, Dipartimento di Matematica "F. Brioschi"
Politecnico di Milano, Via Bonardi 9 - 20133 Milano (Italy)

mox@mate.polimi.it http://mox.polimi.it

Stent deformation, physical stress, and drug elution obtained with provisional stenting, conventional culotte and Tryton-based culotte to treat bifurcations: a virtual simulation study.

Stefano Morlacchi[1,2], M.Eng; Claudio Chiastra[1,2], M.Eng; Elena Cutrì[3], PhD; Paolo Zunino[3,4], PhD; Francesco Burzotta[5], MD; Luca Formaggia[3], PhD; Gabriele Dubini[1], PhD; Francesco Migliavacca[1], PhD.

November 9, 2012

[1] LABS–Laboratory of Biological Structure Mechanics
Structural Engineering Department
Politecnico di Milano, Milan, Italy
[2] Bioengineering Department
Politecnico di Milano, Milan, Italy
[3] MOX– Modeling and Scientific Computing
Department of Mathematics "F. Brioschi"
Politecnico di Milano, Milan, Italy
[4] Department of Mechanical Engineering and Materials Science
University of Pittsburgh, PA, USA
[5] Department of Cardiovascular Medicine
Università Cattolica del Sacro Cuore, Rome, Italy

Keywords: Coronary Bifurcations, Finite Element Analysis, Dedicated Stents, Drug Eluting Stents.

Abstract

Aims: To investigate the possible influence of different bifurcation stenting techniques on stent deformation, physical stress, and drug elution using an implemented virtual tool that comprehends structural, fluid dynamics and drug-eluting numerical models. Methods and results: A virtual bench test based on explicit dynamic modelling was used to simulate procedures on bifurcated coronary vessels performed according to three different stenting techniques: provisional side branch stenting, culotte and Tryton-based culotte. Geometrical configurations obtained after stenting were used to perform fluid dynamics and drug elution analyses. Results show that major different pattern of mechanical deformation, shear stress and theoretical drug elution are obtained using different techniques. Compared with conventional culotte, the dedicated Tryton seems to facilitate the intervention

in terms of improved access to the main branch and lowers its biomechanical influence on the coronary bifurcation in terms of mechanical and hemodynamic parameters. However, since the Tryton stent is a bare metal stent, the drug elution obtained is lower. Conclusion: Numerical models might successfully complement the information on stenting procedures obtained with traditional approaches as in vitro bench testing or clinical trials. Devices dedicated to bifurcations may facilitate procedure completion and may result in specific patterns of mechanical stress, regional blood flow and drug elution.

Abbreviation: MB (Main Branch); SB (Side Branch); DES (Drug-Eluting Stent); BMS (Bare Metal Stent); CFD (Computational Fluid Dynamics); PEEQ (Plastic equivalent deformation); FKB (Final Kissing Balloon); PSB (Provisional Side Branch); WSS (Wall Shear Stress; TAWSS (Time-averaged WSS); RRT (Relative Residence Time); OSI (Oscillatory Shear Index).

1 Introduction

Despite current technical and clinical improvements, bifurcated coronary artery lesions still remain an open challenge for interventional cardiologists performing percutaneous coronary interventions. The "optimal" procedure of stent implantation in bifurcated lesions is still not defined but should theoretically restore both main branch (MB) and side branch (SB) patency, avoiding major myocardial injury and allowing a simple and straight execution. Among the different controversies related to the optimal technique, a major issue is the choice between a single- and a double-stenting approach. At present, available clinical data on bare metal stents (BMS) and drug-eluting stents (DES) suggest that simple strategies are associated with lower rates of adverse clinical events while increased procedure duration, fluoroscopy times and contrast volume affect complex strategies. As a consequence, in most of the cases single-stent provisional technique should be considered as the preferred strategy [1]. However, such evidences stem from studies using standard DES and may be challenged by novel technical innovations such as stents dedicated to bifurcations [2]. These devices may provide new treatment options by solving a series of technical problems related to the implantation of regular stents in bifurcated lesions. Among the different dedicated devices, the Tryton Side Branch stent (Tryton Medical, Durham, NC, USA), has been tested in clinical ground obtaining promising results [3],[4]. It is a balloon-expandable cobalt-chromium BMS characterized by three different specific designs which are designed to facilitate culotte technique. During the evaluation of novel interventional devices, virtual modelling techniques based on numerical methods are emerging as a valuable tool for the assessment of several mechanical (arterial wall and stent struts stresses) [5]-[8] and hemodynamic variables (shear stresses, drug release) [9]-[12] which are

hardly detectable by means of in vitro or in vivo experiments. Accordingly, virtual simulations may be applied to investigate the influence of stenting procedures in coronary bifurcations by implementing a virtual tool that comprehends structural [13], computational fluid dynamics (CFD) [14],[15] and drug-eluting [16] numerical models. Since the physiological consequences of dedicated stents deployment in bifurcated lesions are scarcely investigated, we designed the present study aimed to assess the results obtained with provisional side branch (PSB) stenting procedure, with standard stent-based ("conventional") culotte and Tryton-based culotte using an articulated virtual simulation tool.

2 Methods

In the present study, a sequential implementation of three different numerical models, each one investigating a specific biomechanical aspect of stenting procedures in coronary bifurcations, has been developed and applied. First, a structural model simulating the stent expansions in hyperelastic coronary bifurcations [13] was used to provide insights on the stress fields in both the arterial wall and the implanted devices. Afterwards, the obtained realistic geometries have been used to investigate the hemodynamic influence of stenting procedures on the blood flow [14]-[15]. Finally, the patterns of drug delivery to the lumen and the arterial walls have been assessed [16]. Details regarding the main modelling features of these models have been previously published and are summarized in the following sections.

2.1 Virtual bench testing

In a virtual bench test, structural analyses were implemented to simulate stenting procedures and obtain important biomechanical quantities such as stresses and deformations. This model [13] is based on the solution of an explicit dynamics problem by means of ABAQUS/Explicit commercial code (Dassault Systemes Simulia Corp., RI, USA) and involves three main entities: a three-layered hyperelastic bifurcated artery, elastic angioplasty balloon models and elasto-plastic metallic stents (Fig. 1). The internal diameters of the bifurcation respected the ratios proposed by the Murray law [17] and were 3.28 mm, 2.78 mm and 2.44 mm for the proximal part of the MB, the distal part of the MB and the SB, respectively. The vessel wall was characterized by a constant thickness of 0.9 mm and the bifurcation angle was 45° . Angioplasty balloons, modelled to behave according to the typical dilation performance of semi-compliant balloons, had a diameter of 3 mm for MB and 2.5 mm for SB, respectively. The two examined stents were designed to resemble the Xience V DES system (Abbott Laboratories, Abbott Park, IL, USA) and the dedicated Tryton Side Branch Stent (Tryton Medical, Durham, NC, USA) (BMS). Stent dimensions are shown in Fig. 1. Positions of the devices, specific boundary conditions and pressure

loads have been accurately defined in order to replicate the following stenting procedures [18]:

1. PSB stenting (PSB): a Xience V stent platform crimped to an external diameter of 1.2 mm was positioned across the bifurcation and implanted by inflating a 3 mm balloon at 15 atm. After deployment, final kissing balloon (FKB) inflation was simulated by simultaneous inflation of a 3 mm balloon in the MB and a 2.5 mm balloonin the SB (accessing the SB through the more distal strut available at SB ostium).

2. Conventional culotte (CUL): a Xience V stent, crimped to an external diameter of 1.2 mm, was implanted across the proximal part of the MB and the SB; then, access to distal MB was achieved by expanding a 3 mm balloon through side cells of the SB stent struts. Afterwards, a second Xience V stent was implanted in the MB across the SB take off. Procedure was ended by a FKB inflation using a 3 mm balloon in the MB and a 2.5 mm balloon in the SB.

3. Tryton-based culotte (TRY-CUL): the Tryton stent, crimped to an external diameter of 1.2 mm, was implanted across the proximal part of the MB and the SB; access to distal MB was obtained by opening the SB stent struts with a 3 mm angioplasty balloon. Then, a Xience V stent was implanted in the MB across the SB take off. Procedure was ended by a FKB inflation using a 3 mm balloon in the MB and a 2.5 mm balloon in the SB [19].

As an example of the virtual bench testing modelling used, the complete simulation of the Tryton-based culotte is provided in Figure 2 and Video 1. After virtual bench testing, the metal-to-artery ratios (ratio between the total area of the external surfaces of the stents and the area) at the level of the proximal segment of MB and the plastic equivalent deformations (PEEQ) have been calculated and compared between the three investigated stenting technique to evaluate, respectively, the effects of stent overlap and the specific stent deformations. Additionally, since procedural pitfalls during complex bifurcation stenting procedures may play a major role, we sought to investigate the role of SB rewiring site (a well-established major issue during provisional technique) on culotte techniques. Thus, a thorough investigation of this aspect is carried out in this paper. Optimal rewiring should allow the deployment of the second device and maintain free access to both branches, reducing potential procedural complications. Investigation of this issue is performed by evaluating the cross-sectional area available for an optimal rewiring in case of CUL and TRY-CUL technique. While conventional stents have a regular strut pattern, Tryton performances may be influenced by its asymmetric design and cases of Tryton rotated by 30° and 60° (worst scenario possible) were investigated as well.

2.2 Fluid dynamic Model

The final geometrical configurations obtained by virtual bench testing in the coronary bifurcation were used to create the fluid volume for CFD analyses (Fig. 3) [14],[15]. CFD simulations were focused on near-wall analyses. Blood was defined as an incompressible, non-Newtonian fluid using the Carreau model proposed by Seo et al. [20]. A no slip condition was applied between the fluid and the arterial walls which are assumed to be rigid. A transient velocity profile measured by Davies et al. [21] in a human left anterior descending artery was applied with a constant 70:30 flow split between the MB and SB. Assessment of the velocity field, wall shear stresses (WSS) and relative residence time (RRT) [22] in the stented regions was obtained as follows:

$$RRT = \frac{1}{(1-2\cdot OSI)\cdot TAWSS}$$

where OSI [23] is the oscillatory shear index and TAWSS is the time-averaged WSS. RRT can be associated to the residence time of the particles near the wall. Moreover it has a more tangible connection to the biological mechanisms underlying atherosclerosis than WSS and OSI [22],[24]. Low WSS and high RRT are recognized as critical for the problem of atherogenesis and in-stent restenosis [25],[26].

2.3 Drug-eluting models

In complex lesions such as coronary bifurcations [27], understanding the capabilities of eluting anti-proliferative drug becomes essential in the assessment of different stenting procedures. Starting from the deformed configurations obtained via structural analysis, a computational model to perform the coupled analysis of fluid dynamics and drug release was applied using an in-house code [16],[28]. The model takes into account diffusion and dissolution mediated drug release process with finite dissolution rate according to the equations proposed in Frenning et al. [29]. More precisely, drug dissolves and diffuses through the interstices of the DES coating in order to finally reach the outer surface and be released. For drug transport into the arterial walls, drug diffusion and binding as well as arterial leakage are relevant phenomena [30]. A fully coupled steady simulation of blood flow and intramural plasma filtration was performed with this purpose. The obtained pressure and velocity field were then used to perform the analysis of drug release. According to the model proposed in DAngelo et al. [31] the drug concentration inside the lumen is governed by an advection, diffusion model. Drug absorption in the arterial wall is described by means of an advective-diffusive model as for the lumen complemented by a reaction term accounting for dynamic binding of the drug to the extracellular matrix [32],[33]. The drug diffusion coefficient refers to release of heparin[34]. For the stent struts we assumed a squared section 0.08 mm wide (which is coherent with the selected

stent platform, see Sheiban et al. [35]). As a result of that, the equivalent radius is equal to 0.052 mm. The coating consists of a polymeric film with a thickness of 7 μm. In order to evaluate the drug delivery to the arterial wall, we addressed the dose, which is defined as the time-averaged drug concentration at each point of the arterial wall, and its mean value over a given control volume. The drug doses for the whole region of the coronary bifurcation domain and for three meaningful sub-regions, namely the proximal part of the MB, the distal part of the MB and the SB region, were evaluated.

3 Reults

3.1 Geometrical configurations and physical deformations

Figure 4 shows the final geometrical configurations obtained at the end of virtual bench testing. Since all simulated procedures included optimal (distal) SB rewiring and FKB inflation, all the procedures resulted in patent accesses to both the MB and SB. Metal to artery ratios in the proximal region of the MB are shown in Fig. 5. In the PSB approach only one stent is implanted resulting in a metal-to-artery ratio equal to 13.2%. On the other hand, when two conventional devices are implanted as in CUL, the ratio increases to 27.4%. In case of TRY-CUL, the use of the dedicated stent, thanks to the fewer struts in its proximal design, reduces the ratio to 20.6%. Regarding stent deformation assessment, the maximum PEEQ obtained at the end of the procedures in the three simulated techniques are reported in Fig. 6. In case of PSB stenting, results showed that the maximum deformation value (0.75) is obtained in the stent strut at the ostium of the SB opened during the FKB inflation. This final step also influences the deformation state of the in the proximal part of the MB stent by increasing the max values of PEEQ from 0.33 to 0.43. Similar values of deformations can be found in the MB stents deployed in cases CUL and TRY-CUL. On the other hand, looking at the plastic equivalent deformations induced in the stents implanted from the proximal MB toward the SB in the two culotte techniques, we found that the conventional stent used in CUL undergoes very high deformations in the strut opened toward the MB (0.95) while the dedicated stent used in the TRY-CUL has overall lower deformation with its higher deformation values (0.65) at the ring of struts located at its proximal end.

3.2 Fluid dynamic analyses: WSS and RRT

Fluid dynamic analyses disclosed significant differences between the three investigated technique at the level of proximal MB. Figure 7 depicts the contour maps of the TAWSS (left) and RRT (right) in the three cases examined. Overall, contour maps for both parameters concordantly showed that better shear stress pattern in the proximal MB is obtained with PSB (single layer of stent struts) while the (higher or lower amount of) double metallic layers associated (respec-

tively) with the CUL and TRY-CUL has a adverse impact on shear stresses by enhancing the areas with low shear stress. In particular, numerical TAWSS analysis showed that the percentage areas of the proximal part of MB characterized by TAWSS lower than 0.25 Pa were 56.0%, 88.1% and 71.6% for PSB, CUL and TRY-CUL, respectively. Similar results were obtained in the RRT analysis (Figure 7, numerical data not shown).

3.3 Theoretical drug elution capability

For each stenting procedure, the total amount of drug concentration in the arterial wall is reported in Fig. 8 at different time instants. The drug supply to the arterial wall increases until 6 hours and then a decrease is observed since the total amount of drug in the stent coating is completely released. The mean dose was quantified and displayed in the histograms of Fig. 9 considering the different bifurcation areas. Reported graphics show that major differences in the pattern of drug release are obtained with the three investigated techniques. In particular, it is evident how drug release in the SB is only effective after the implantation of a DES. Furthermore, strut distribution and different stent designs have been shown to highly affect the drug concentration in the arterial walls, especially in the proximal MB where multiple metallic layers occur. The comparison of these values between PSB, conventional and Tryton-based culotte configurations has been more thoroughly discussed in the next section.

3.4 SB stent rewiring: importance of a dedicated design

SB stent rewiring may have a major role in culotte techniques. The available areas for optimal re-crossing of the device are equal to 8.7% after Xience V deployment and 59.4%, 47.6% and 40.8% for the three deployments of Tryton (ideal case, rotation 30° and rotation 60° , respectively) (Fig. 10). Following, the expansion of a MB balloon results in a patent access to MB in all these cases. As a consequence, the dedicated stent seems to facilitate rewiring. Instead, procedural complications due to sub-optimal re-crossing of a conventional stent seem to be more feasible and may lead to negative geometrical and hemodynamic conditions as illustrated in Fig. 11. This case is discussed in more details in the next section.

4 Discussion

The combination of the results obtained from the three numerical models previously described provides new insights on several aspects of the treatment of coronary bifurcations with single- or double-stenting procedures, conventional or dedicated devices. Tryton stent is characterized by fewer struts in its proximal part and is designed to overcome some of the procedural complications

that affect double stenting techniques as, for instance, wide double metallic layers or problematic accesses with the second device. Firstly, a critical point of double-stenting procedures, particularly evident in the culotte techniques, is the occurrence of double or even triple metallic layers [36]. These issues might result in higher metal-to-artery ratios, indication of a biomechanical environment more disposed to arterial wall injuries and post-stenting complications. In this work, the three cases investigated show very different metal-to-artery ratios in the proximal part of the MB where the double metallic layer occurs (Fig. 5). In particular, the PSB approach results in the lowest metal-to-artery ratio since only one stent is implanted. On the other hand, when two conventional devices are implanted as in the conventional culotte, the ratio doubles. The use of Tryton SB stent, thanks to the fewer struts in its proximal design, reduces this ratio to 20.6%. The presence of a double-metallic layer has a negative influence on the hemodynamic field as well, as proved by the fluid dynamic results illustrated in Fig. 7. Low values of WSS are considered as risk factors of in-stent restenosis and, as a consequence, should be avoided [25]. TAWSS magnitude contour maps of the three cases confirm that the presence of stent struts provokes a decrease of the WSS acting on the arterial wall; this is particularly evident in the regions characterized by the overlapping of the two stents as in case of conventional culotte. If compared to this case, the dedicated device improves the hemodynamic conditions by decreasing the percentage of areas with low WSS from 88.1% of case 2 to 71.6%.Another critical issue is that conventional devices are designed to reach stresses and deformations that might be potentially exceeded during challenging techniques used in complex geometries such as coronary bifurcations. This occurrence might undermine the mechanical integrity of the devices. Beyond structural integrity and potential stent fracture, other important drawbacks have been related to the high deformations achieved during the expansions. Previous reports [37] show that very high deformations in the device might lead to structural damage and delamination of the polymer that covers the stent struts and carries anti-proliferative drugs. Polymer delamination could bring to an inhomogeneous distribution of the eluted drug disturbing the correct healing process of the artery. Indeed, structural simulations show that in all the cases, very high stresses and PEEQ are found in the conventional devices deployed (Fig. 6). In particular, looking at the MB stent, high plastic deformations are found in all those stent struts rewired with a SB angioplasty balloon and opened during FKB inflations. However, these values, ranging from 0.61 to 0.77, are lower than those obtained in case of conventional culotte after the re-crossing of the SB stent with a 3 mm balloon dilated in the MB. PEEQ values are equal to 0.95 and localize at the strut hinges close to the arterial wall opposite to the bifurcation. The same step does not seem to be such critical in case of Tryton-based culotte since lower values of stresses and PEEQ (around 0.65) are found in the dedicated device deployed in the SB. This occurrence proves that a dedicated design might be needed to decrease the mechanical solicitations in the devices. In the DES era, the capability of eluting drug has

become an essential requirement for coronary stents. Since in vitro or in vivo investigation of this aspect is technically very complex and demanding, numerical models started to be exploited and proved their ability of assessing drug delivery in the arterial wall [16],[28], [30]. In this work, the numerical models described in section 2.3 have been applied to the three cases investigated (Fig. 8 and 9). The comparison among the configurations gives rise to interesting considerations. First, a higher drug dose is observed in the conventional culotte procedure with respect to the PSB, but the drug dosage is not doubled. Indeed, the incomplete stent apposition and the struts superposition occurring in the case of a double-stenting procedure affect the optimal release of drug to the arterial wall causing drug loss in the blood stream. Concerning the SB region, an adequate drug supply seems to be provided only in the case when the SB is treated by means of a DES (conventional culotte). A small supply of drug in the SB is observed in the other cases and it is probably due to the flow mediated drug transport. The use of a dedicated BMS in the SB guarantees the re-opening of the stenotic area but seems not to be able to supply a sufficient amount of drug to the SB. These results are in agreement with the considerations by Grundeken et al. [2], who suggested that further improvements might be achieved by coating these dedicated SB devices with a drug, with the aim of not only providing an optimal ostial scaffolding of the SB but also minimizing the in-stent restenosis. Moreover, the presence of bare/metal struts in the proximal segment of the MB seems to influence the pattern of drug release at this level after TRY-CUL. Lastly, it is quite reasonable to assume that sub-optimal procedural outcomes could increase the potential risks of post-stenting clinical complications as in-stent restenosis or thrombosis. Above all, double-stenting procedures seem to be more prone to experience procedural errors mainly due to their technical complexity. In particular, within the culotte techniques a critical point is the crossing of the first device implanted with an angioplasty balloon that enlarges the stent struts and allows the advancement of the second device in the other branch. An optimal balloon insertion should cross the SB stent close to the bifurcation to let the struts adhere to the arterial wall opposite to the bifurcation without hindering the SB access. Looking at the virtual bench test results in Fig. 10, it is clear that the dedicated stent provides a wider area (59.4%) available for an optimal re-crossing (Fig. 10b) if compared to the standard stent (8.7%) (Fig. 10a). Moreover, the highly regular structure of the conventional stent makes the optimal crossing area slightly affected by the uncontrollable rotation of the device. On the other hand, a sub-optimal procedure performed with the Tryton stent rotated of 30° (Fig. 10c) and 60° (Fig. 10d) (worst scenario) reduces the crossing area to 47.6% and 40.8% respectively, still enhancing the performances of the conventional device examined. In all these cases, the following MB balloon inflation results in a completely patent access to MB (Fig. 10, bottom), thus making rotational alignment of the Tryton SB stent a trivial point. Accordingly, the use of a dedicated device seems to have lower chances of procedural complications due to sub-optimal SB stent rewiring. On the other hand, sub-optimal rewiring

of a conventional SB stent seems to be more probable and, when occurring, may lead to negative geometrical and hemodynamic conditions. For instance, Fig. 11 provides a comparison between an optimal conventional CUL technique (Fig. 11-left) and an example of sub-optimal procedure obtained crossing the stent struts far from the bifurcation (Fig. 11-right). In the second case, the result of the MB balloon deployment is a patent MB ostium but a problematic access to SB caused by the presence of several stent struts. In this way, after the MB stent deployment, FKB inflation could only be performed with a proximal access to SB, leading to a greater new metallic carina. Results in terms of geometrical configuration and hemodynamic influence at the end of the whole procedure are visible in Fig. 11b and 11c, respectively. In particular, differences can be found looking at the longer new metallic carina obtained in the sub-optimal case (3.95 mm) respect to the optimal one (2.65 mm). This new metallic carina has a great influence on the hemodynamic field as proved by the CFD results shown in Fig. 11c. In particular, a wider area of low velocities and recirculations is visible close to the bifurcation. Slight increases in the mechanical solicitations on the devices in terms of Von Mises stresses and plastic deformations at the maximum expansion were found as well.

5 Study limitations

Despite their continuous improvements and upgrading, numerical models are still affected by a number of limitations that need to be overcome to fully replicate in vivo clinical conditions. In the following paragraph, some of the assumptions made are listed:

- Artery: the materials used to define its mechanical behaviour do not consider its anisotropic and inhomogeneous nature. The geometries used in this work have realistic dimensions but only represent idealized models.
- Atherosclerotic plaques have not been included in the model.
- Stent models could slightly differ from the actual commercial devices. Moreover, only a single conventional stent has been investigated.
- No image-based reconstructions have been used. Indeed the models implemented cannot provide patient-specific indications but only general guidelines that must be carefully interpreted and adapted to every specific clinical case.

6 Conclusions

This work shows how numerical models might successfully complement the information on stenting procedures obtained with traditional approaches as in vitro

bench testing or clinical trials. Their ability of providing direct information on clinically interesting biomechanical variables such as mechanical stresses in the artery and the stents could facilitate design process of the devices and clinical planning. In particular, this work confirmed that new dedicated devices, still requiring some improvements in their design and concept, might be an interesting opportunity while stenting coronary bifurcation lesions.

7 Acknowledgments

The authors have been supported by the Grant Nanobiotechnology: Models and methods for degradable materials of the Italian Institute of Technology (IIT). The authors E. Cutrì, L. Formaggia and P. Zunino are also supported by the European Research Council Advanced Grant Mathcard, Mathematical Modelling and Simulation of the Cardiovascular System, Project ERC-2008-AdG 227058. The authors S. Morlacchi, C. Chiastra, G. Dubini and F. Migliavacca are also supported by the European Commission under the 7th Framework Programme, within the project RT3S - Real Time Simulation for Safer vascular Stenting.

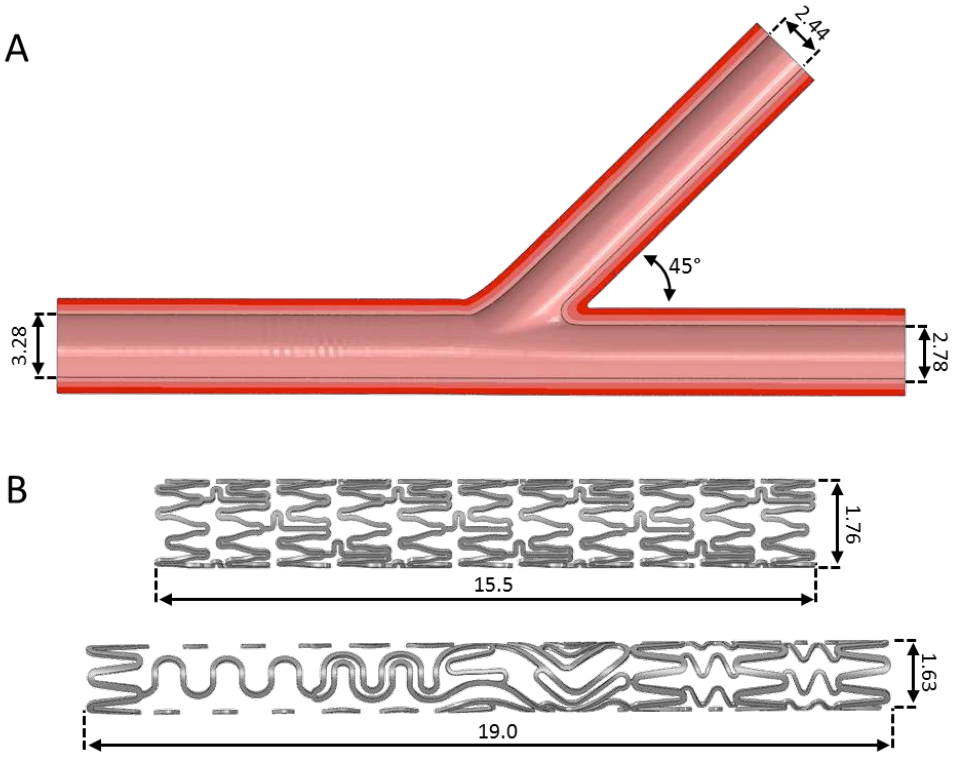

Figure 1: A) 3D model of the coronary bifurcation respecting the dimensional Murray law; B) CAD model of the two stents investigated: the conventional stent Xience V (top) and the dedicated device Tryton Side Branch stent (bottom). All measures reported are in millimetres.

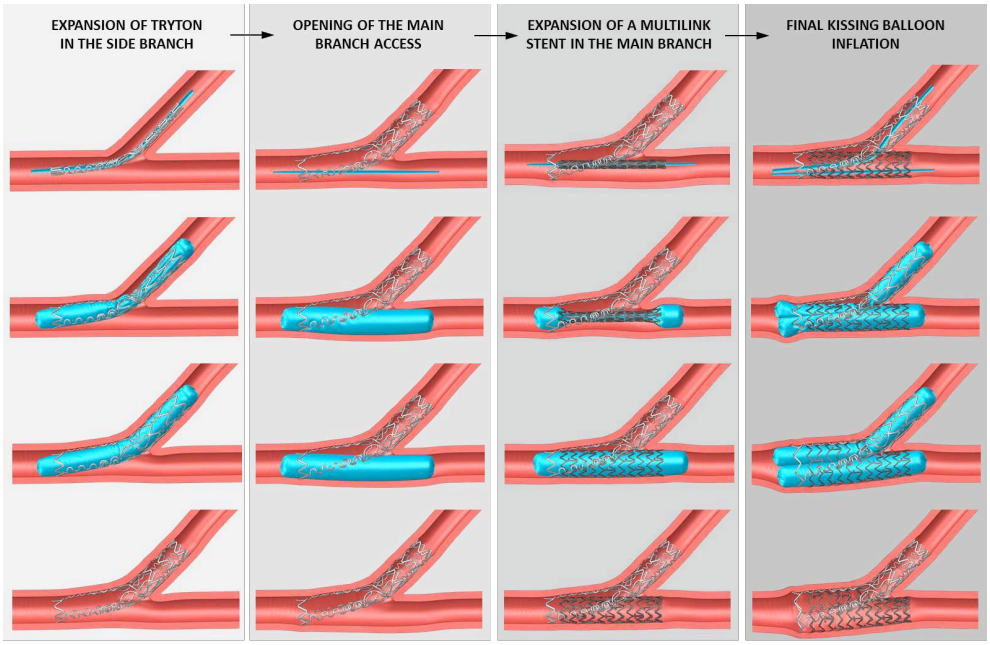

Figure 2: Virtual structural simulation of the Tryton-based culotte technique: implantation of the Tryton stent in the SB with a 2.5 mm balloon; opening of the MB using a 3 mm balloon; expansion of a conventional Xience V stent in the MB with a 3 mm balloon; FKB inflation performed with a 2.5 mm balloon in the SB and a 3 mm balloon in the MB.

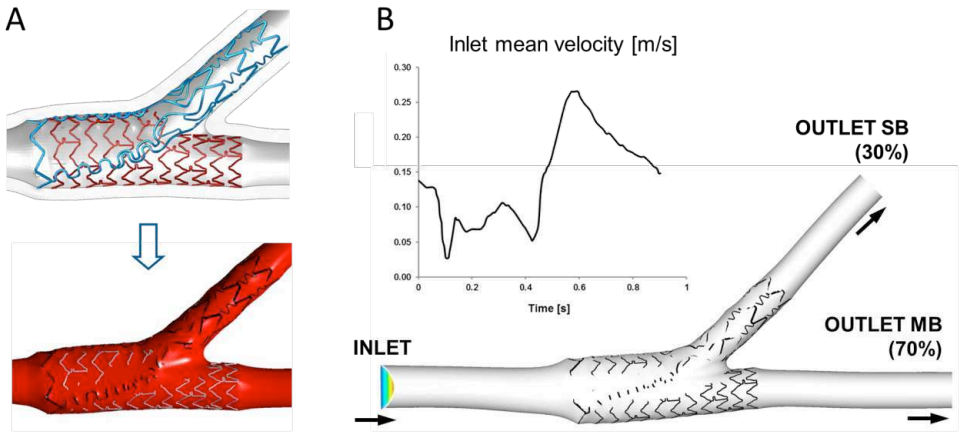

Figure 3: A) Definition of the fluid volume after the structural expansion of Case 3. B) CFD model and velocity tracing applied at the inlet section of the bifurcation.

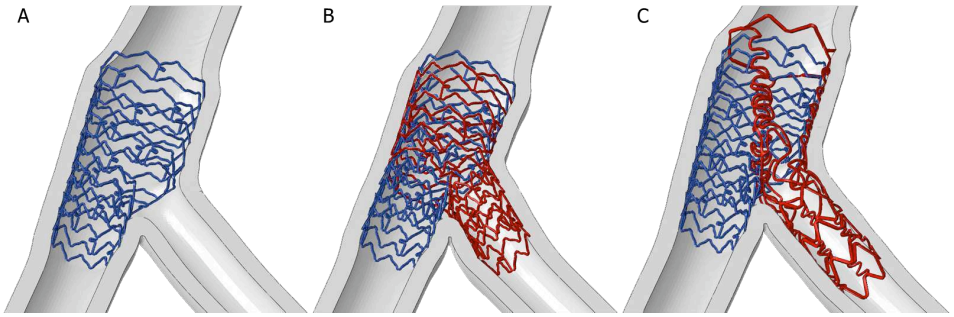

Figure 4: Final deformed geometrical configurations at the end of the three simulated procedures: A) Provisional Side Branch stenting (PSB); B) culotte technique performed with two conventional stents (CUL); C) culotte technique performed with a conventional Xience V stent in the MB and the Tryton stent in the SB (TRY-CUL).

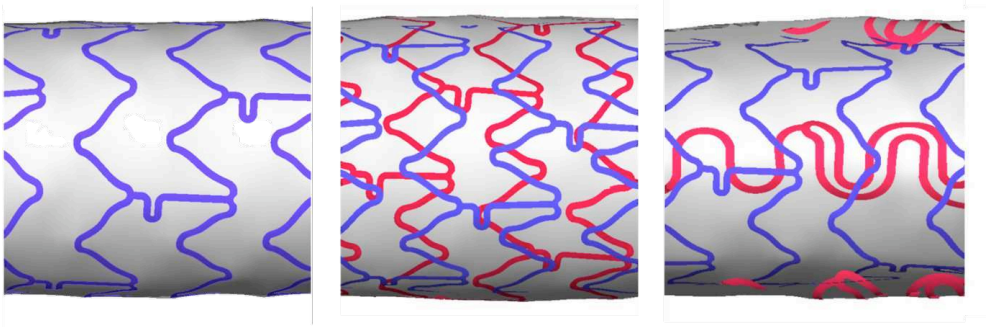

Figure 5: Metal-to-artery ratios for the three cases investigated: PSB (left), CUL (middle) and TRY-CUL (right). The measured ratios in the same region of the proximal MB are 13.2%, 27.4% and 20.6%, respectively.

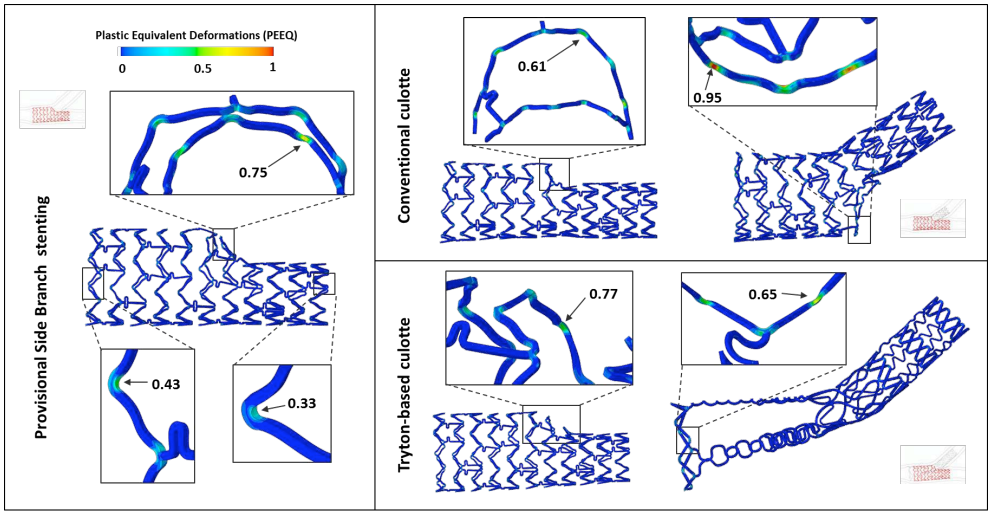

Figure 6: Comparison between the plastic equivalent deformations (PEEQ) obtained at the end of the stenting procedures in case of PSB stenting (left), CUL (right, top) and TRY-CUL (right, bottom). Magnification areas show maximum values obtained in the devices implanted.

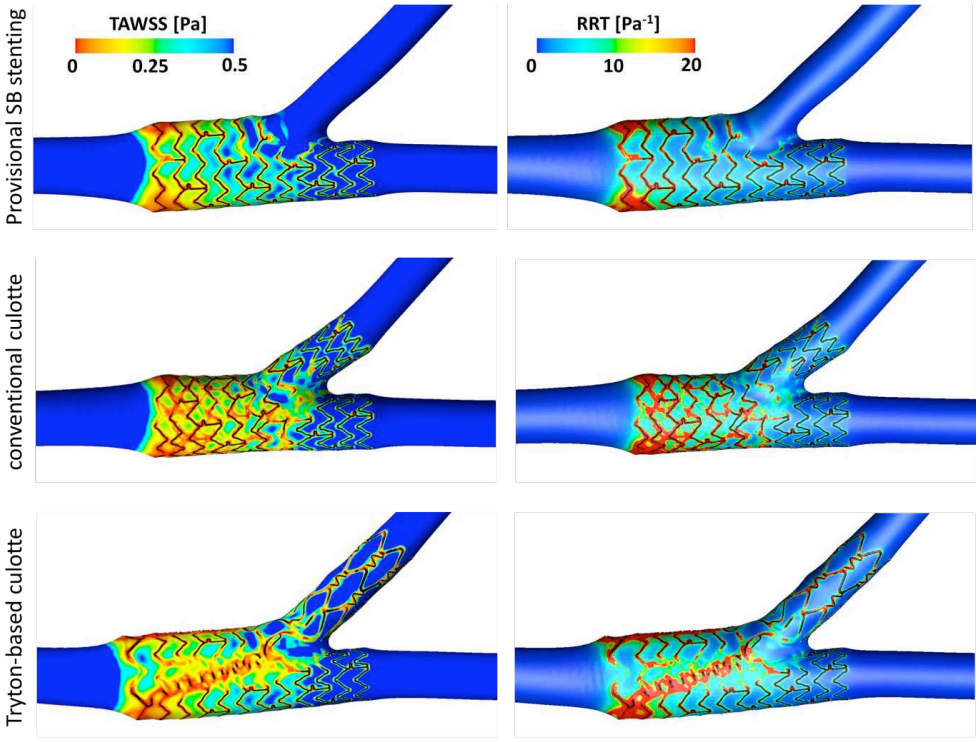

Figure 7: TAWSS and RRT contour maps: comparison between PSB stenting (top), CUL (middle) and TRY-CUL (bottom).

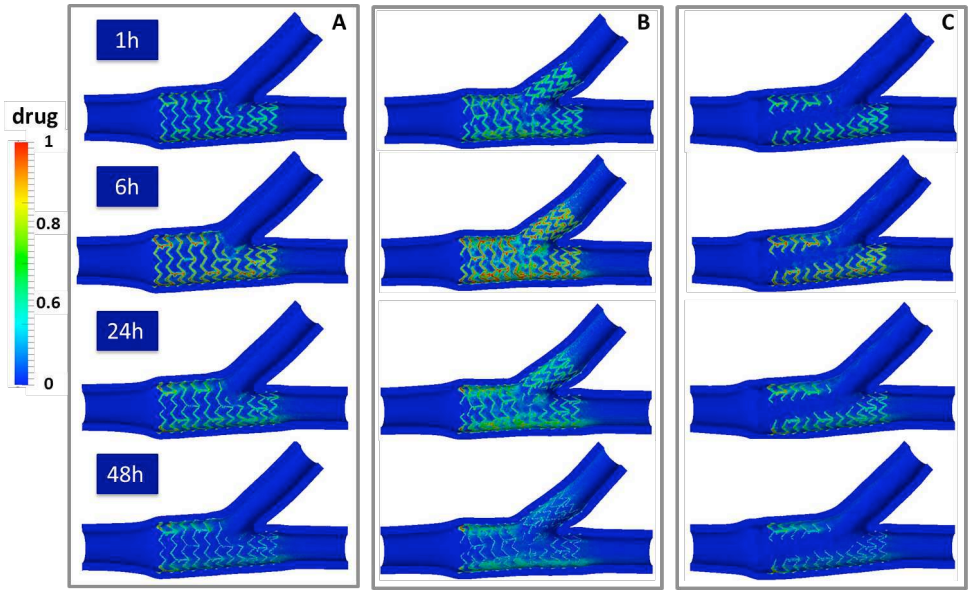

Figure 8: Drug distribution in the arterial wall of the coronary bifurcation evaluated at different time instants (1h, 6h, 24h, 48h) for the PSB stenting (A), conventional CUL (B) and TRY-CUL technique (C).

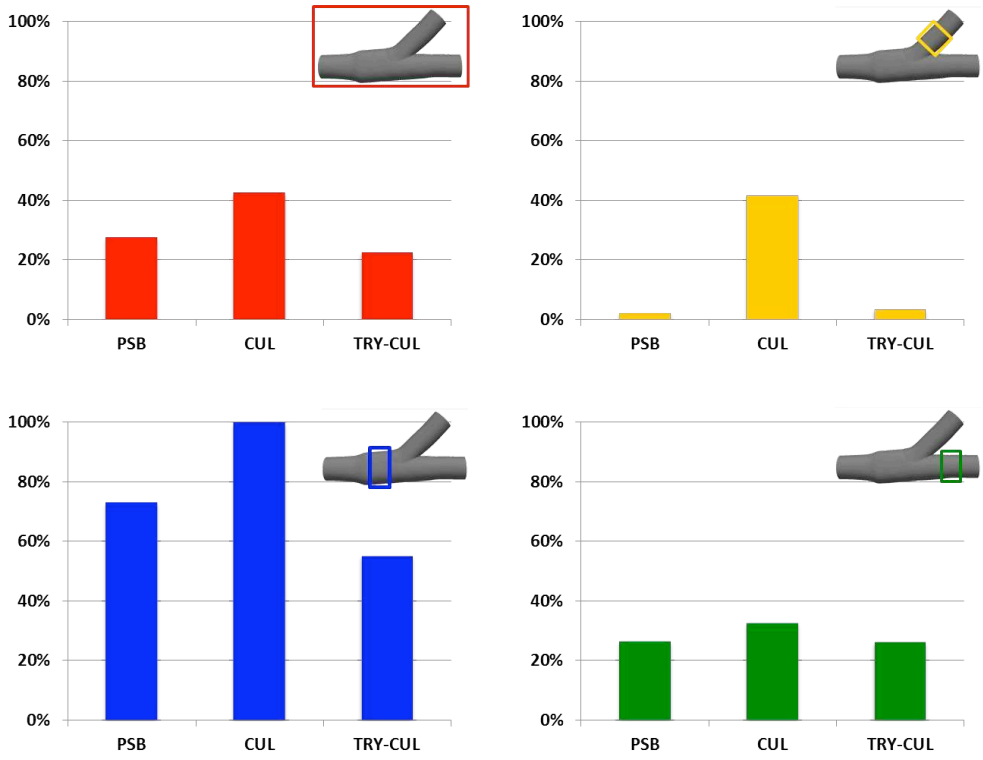

Figure 9: Mean drug dose evaluated for the whole bifurcation (red) and for the proximal (blue), distal (green) and side branch portions (yellow) for the three investigated procedures. The values are normalized with respect to the maximum value of the dose.

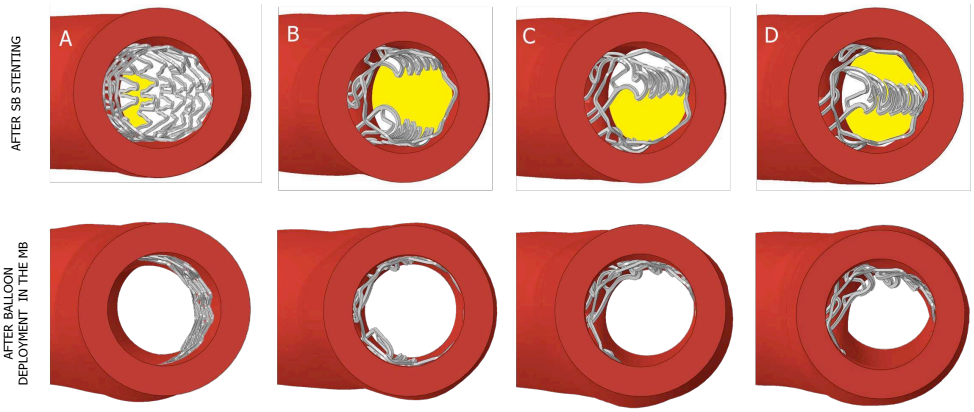

Figure 10: Top) Different accesses to MB after SB stent expansion with a 2.5 mm balloon: deployment of the conventional Xience V stent (A); implantation of the Tryton SB stent in the ideal configuration (B) and rotated of 30° (C) and 60° (D), the worst possible scenario. Yellow areas represent the available area for optimal re-crossing of the device and are equal to 8.7%, 59.4%, 47.6% and 40.8%, respectively. Below) Geometrical configurations after the deployment in the MB of a 3 mm balloon.

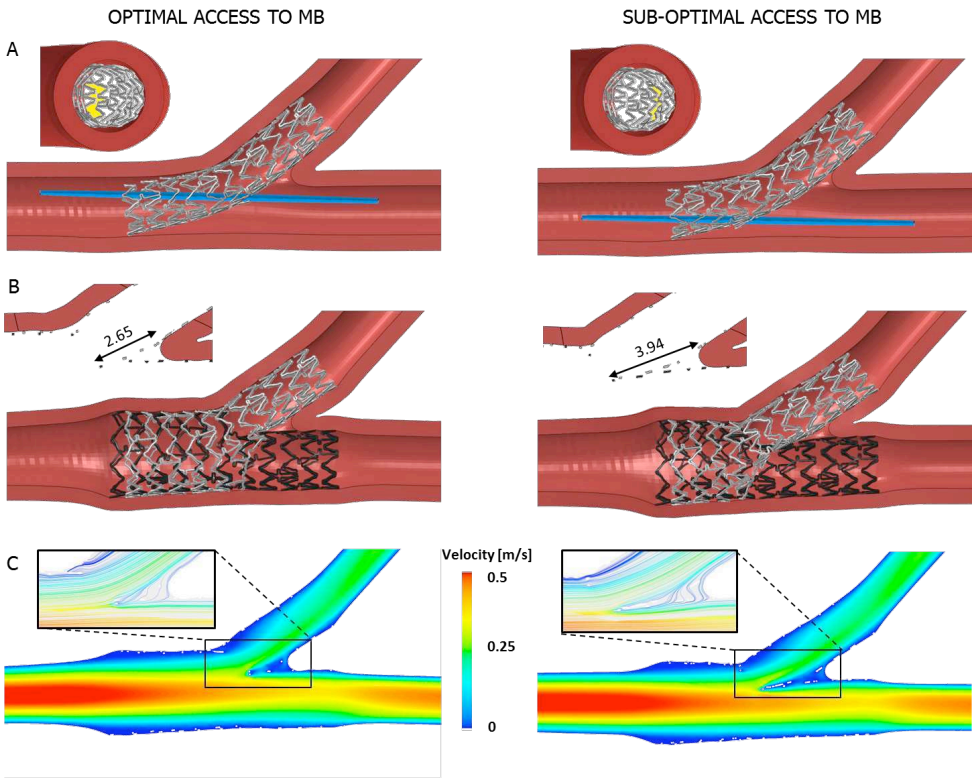

Figure 11: Comparison between an optimal and a sub-optimal access to MB in case of conventional CUL. A) Optimal (left) and sub-optimal (right) crossing of the device with an angioplasty balloon. In the views from the proximal part of the MB, the crossing area is highlighted in yellow. B) Final configuration of the devices after the conventional c technique. A longer new metallic carina is obtained with the sub-optimal access, as underlined in the close-ups of the transversal planes. C) Velocity magnitude contour maps at the maximum flow rate: in the magnification areas, the low velocities and more disturbed flow provoked by the longer metallic carina are visible.

References

[1] D. Hildick-Smith, J. Lassen, R. Albiero, T. Lefevre, O. Darremont, M. Pan, M. Ferenc, G. Stankovic, and Y. Louvard. Consensus from the 5th european bifurcation club meeting. *EuroIntervention*, 6(1):34–38, 2010.

[2] M. Grundeken, P. Stella, and J. Wykrzykowska. Why the provisional single-stent approach is not always the right strategy; arguments for the development of dedicated bifurcation devices. *EuroIntervention*, 7(11):1249–1253, 2012.

[3] M. Magro, J. Wykrzykowska, P. Serruys, C. Simsek, S. Nauta, M. Lesiak, K. Stanislawska, Y. Onuma, E. Regar, R. Van Domburg, S. Grajek, and R. Geuns. Six-month clinical follow-up of the tryton side branch stent for the treatment of bifurcation lesions: A two center registry analysis. *Catheterization and Cardiovascular Interventions*, 77(6):798–806, 2011.

[4] P. Agostoni, D. Foley, M. Lesiak, A. Belkacemi, J. Dens, I. Kumsars, B. Scott, P. Oemrawsingh, C. Dubois, E. Garcia, T. Lefévre, and P. Stella. A prospective multicentre registry, evaluating real-world usage of the tryton side branch stent: Results of the e-tryton 150/benelux registry. *EuroIntervention*, 7(11):1293–1300, 2012.

[5] C. Capelli, F. Gervaso, L. Petrini, G. Dubini, and F. Migliavacca. Assessment of tissue prolapse after balloon-expandable stenting: Influence of stent cell geometry. *Medical Engineering and Physics*, 31(4):441–447, 2009.

[6] P. Mortier, M. De Beule, P. Segers, P. Verdonck, and B. Verhegghe. Virtual bench testing of new generation coronary stents. *EuroIntervention*, 7(3):369–376, 2011.

[7] P. Mortier and M. De Beule. Stent design back in the picture: An engineering perspective on longitudinal stent compression. *EuroIntervention*, 7(7):773–775, 2011.

[8] F. Harewood, J. Grogan, and P. McHugh. A multiscale approach to failure assessment in deployment for cardiovascular stents. *Journal of Multiscale Modeling*, 2(1-2):1–22, 2010.

[9] S. Morlacchi, B. Keller, P. Arcangeli, M. Balzan, F. Migliavacca, G. Dubini, J. Gunn, N. Arnold, A. Narracott, D. Evans, and P. Lawford. Hemodynamics and in-stent restenosis: Micro-ct images, histology, and computer simulations. *Annals of Biomedical Engineering*, 39(10):2615–2626, 2011.

[10] A. Williams, B. Koo, T. Gundert, P. Fitzgerald, and J. J. LaDisa. Local hemodynamic changes caused by main branch stent implantation and subsequent virtual side branch balloon angioplasty in a representative coronary bifurcation. *Journal of Applied Physiology*, 109(2):532–540, 2010.

[11] L. Ellwein, H. Otake, T. Gundert, B. Koo, T. Shinke, Y. Honda, J. Shite, and J. LaDisa Jr. Optical coherence tomography for patient-specific 3d artery reconstruction and evaluation of wall shear stress in a left circumflex coronary artery. *Cardiovascular Engineering and Technology*, 2(3):212–227, 2011.

[12] V. Kolachalama, E. Levine, and E. Edelman. Luminal flow amplifies stent-based drug deposition in arterial bifurcations. *PLoS ONE*, 4(12), 2009.

[13] D. Gastaldi, S. Morlacchi, R. Nichetti, C. Capelli, G. Dubini, L. Petrini, and F. Migliavacca. Modelling of the provisional side-branch stenting approach for the treatment of atherosclerotic coronary bifurcations: Effects of stent positioning. *Biomechanics and Modeling in Mechanobiology*, 9(5):551–561, 2010.

[14] S. Morlacchi, C. Chiastra, D. Gastaldi, G. Pennati, G. Dubini, and F. Migliavacca. Sequential structural and fluid dynamic numerical simulations of a stented bifurcated coronary artery. *Journal of Biomechanical Engineering*, 133(12), 2011.

[15] C. Chiastra, S. Morlacchi, S. Pereira, G. Dubini, and F. Migliavacca. Computational fluid dynamics of stented coronary bifurcations studied with a hybrid discretization method. *European Journal of Mechanics, B/Fluids*, 35:76–84, 2012.

[16] E. Cutrì, P. Zunino, S. Morlacchi, C. Chiastra, and F. Migliavacca. Drug delivery patterns for different stenting techniques in coronary bifurcations: a comparative computational study. *Biomechanics and Modelling in Mechanobiology*, In press, 2012.

[17] C. Murray. The physiological principle of minimum work: I. the vascular system and the cost of blood volume. *Proceedings of the National Academy of Sciences of the United States of America*, 12(3):207–214, 1926.

[18] Y. Louvard, M. Thomas, V. Dzavik, D. Hildick-Smith, A. Galassi, M. Pan, F. Burzotta, M. Zelizko, D. Dudek, P. Ludman, I. Sheiban, J. Lassen, O. Darremont, A. Kastrati, J. Ludwig, I. Iakovou, P. Brunel, A. Lansky, D. Meerkin, V. Legrand, A. Medina, and T. Lefévre. Classification of coronary artery bifurcation lesions and treatments: Time for a consensus! *Catheterization and Cardiovascular Interventions*, 71(2):175–183, 2008.

[19] A. Kaplan and H. Davis. Tryton side-branch stent. *Eurointervention*, 2(2):270–271, 2006.

[20] T. Seo, L. Schachter, and A. Barakat. Computational study of fluid mechanical disturbance induced by endovascular stents. *Annals of Biomedical Engineering*, 33(4):444–456, 2005.

[21] J. Davies, Z. Whinnett, D. Francis, C. Manisty, J. Aguado-Sierra, K. Willson, R. Foale, I. Malik, A. Hughes, K. Parker, and J. Mayet. Evidence of a dominant backward-propagating "suction" wave responsible for diastolic coronary filling in humans, attenuated in left ventricular hypertrophy. *Circulation*, 113(14):1768–1778, 2006.

[22] H. Himburg, D. Grzybowski, A. Hazel, J. LaMack, X.-M. Li, and M. Friedman. Spatial comparison between wall shear stress measures and porcine

arterial endothelial permeability. *American Journal of Physiology - Heart and Circulatory Physiology*, 286(5 55-5):H1916–H1922, 2004.

[23] D. Ku, D. Giddens, C. Zarins, and S. Glagov. Pulsatile flow and atherosclerosis in the human carotid bifurcation. positive correlation between plaque location and low and oscillating shear stress. *Arteriosclerosis*, 5(3):293–302, 1985.

[24] S.-W. Lee, L. Antiga, and D. Steinman. Correlations among indicators of disturbed flow at the normal carotid bifurcation. *Journal of Biomechanical Engineering*, 131(6), 2009.

[25] A. Malek, S. Alper, and S. Izumo. Hemodynamic shear stress and its role in atherosclerosis. *Journal of the American Medical Association*, 282(21):2035–2042, 1999.

[26] Y. Hoi, Y.-Q. Zhou, X. Zhang, R. Henkelman, and D. Steinman. Correlation between local hemodynamics and lesion distribution in a novel aortic regurgitation murine model of atherosclerosis. *Annals of Biomedical Engineering*, 39(5):1414–1422, 2011.

[27] M. Morice, P. Serruys, J. Eduardo Sousa, J. Fajadet, E. Hayashi, M. Perin, A. Colombo, G. Schuler, P. Barragan, G. Guagliumi, F. Molnàr, and R. Falotico. A randomized comparison of a sirolimus-eluting stent with a standard stent for coronary revascularization. *New England Journal of Medicine*, 346(23):1773–1780, 2002.

[28] C. D'Angelo, P. Zunino, A. Porpora, S. Morlacchi, and F. Migliavacca. Model reduction strategies enable computational analysis of controlled drug release from cardiovascular stents? *SIAM Journal on Applied Mathematics*, 71(6):2312–2333, 2011.

[29] G. Frenning. Theoretical investigation of drug release from planar matrix systems: Effects of a finite dissolution rate. *Journal of Controlled Release*, 92(3):331–339, 2003.

[30] B. Balakrishnan, A. Tzafriri, P. Seifert, A. Groothuis, C. Rogers, and E. Edelman. Strut position, blood flow, and drug deposition: Implications for single and overlapping drug-eluting stents. *Circulation*, 111(22):2958–2965, 2005.

[31] C. D'Angelo and P. Zunino. Robust numerical approximation of coupled stokes' and darcy's flows applied to vascular hemodynamics and biochemical transport. *ESAIM: Mathematical Modelling and Numerical Analysis*, 45(3):447–476, 2011.

[32] D. Sakharov, L. Kalachev, and D. Rijken. Numerical simulation of local pharmacokinetics of a drug after intravascular delivery with an eluting stent. *Journal of Drug Targeting*, 10(6):507–513, 2002.

[33] A. Tzafriri, A. Levin, and E. Edelman. Diffusion-limited binding explains binary dose response for local arterial and tumour drug delivery. *Cell Proliferation*, 42(3):348–363, 2009. cited By (since 1996) 11.

[34] C. Hwang, D. Wu, and E. Edelman. Physiological transport forces govern drug distribution for stent-based delivery. *Circulation*, 104(5):600–605, 2001.

[35] I. Sheiban, G. Villata, M. Bollati, D. Sillano, M. Lotrionte, and G. Biondi-Zoccai. Next-generation drug-eluting stents in coronary artery disease: Focus on everolimus-eluting stent (xience v®). *Vascular Health and Risk Management*, 4(1):31–38, 2008.

[36] A. Latib and A. Colombo. Management of bifurcation lesions. *Controversies and Consensus in Imaging and Intervention*, 5(2):C212, 2007.

[37] P. Guerin, P. Pilet, G. Finet, Y. Goueffic, J. N'Guyen, D. Crochet, I. Tijou, P. Pacaud, and G. Loirand. Drug-eluting stents in bifurcations: Bench study of strut deformation and coating lesions. *Circulation: Cardiovascular Interventions*, 3(2):120–126, 2010.

MOX Technical Reports, last issues

Dipartimento di Matematica "F. Brioschi",
Politecnico di Milano, Via Bonardi 9 - 20133 Milano (Italy)

03/2013 Antonietti, P.F.; Ayuso de Dios, B.; Bertoluzza, S.; Pennacchio, M.
Substructuring preconditioners for an $h-p$ Nitsche-type method

04/2013 Morlacchi, S.; Chiastra, C.; Cutr, E.; Zunino, P.; Burzotta, F.; Formaggia, L.; Dubini, G.; Migliavacca, F.
Stent deformation, physical stress, and drug elution obtained with provisional stenting, conventional culotte and Tryton-based culotte to treat bifurcations: a virtual simulation study

02/2013 Brugiapaglia, S.; Gemignani, L.
On the simultaneous refinement of the zeros of H-palindromic polynomials

01/2013 Arnold, D.N.; Boffi, D.; Bonizzoni,F.
Tensor product finite element differential forms and their approximation properties

56/2012 Ieva, F.; Paganoni, A.M.
Risk Prediction for Myocardial Infarction via Generalized Functional Regression Models

55/2012 Peng Chen, Alfio Quarteroni, Gianluigi Rozza
Uncertainty quantification of the human arterial network

54/2012 Ettinger, B., Perotto, S.; Sangalli, L.M.
Spatial regression models over two-dimensional manifolds

53/2012 Fumagalli, A.; Scotti, A.
An efficient XFEM approximation of Darcy flows in fractured porous media

52/2012 Perotto, S.
Hierarchical model (Hi-Mod) reduction in non-rectilinear domains

51/2012 Beck, J.; Nobile, F.; Tamellini, L.; Tempone, R.
A quasi-optimal sparse grids procedure for groundwater flows